JOURNAL OF AGRICULTURAL AND FOOD CHEMISTRY

J. Agric. Food Chem. **2004,** *52,* 7353–7361 **7353**

Using Synchrotron-Based FTIR Microspectroscopy To Reveal Chemical Features of Feather Protein Secondary Structure: Comparison with Other Feed Protein Sources

PEIQIANG YU,*,† JOHN J. MCKINNON,† COLLEEN R. CHRISTENSEN,§ AND DAVID A. CHRISTENSEN†

College of Agriculture, University of Saskatchewan, 51 Campus Drive, Saskatoon, Canada S7N 5A8; and Canadian Light Source, 101 Perimeter Road, Saskatoon, Canada S7N 0X4

Studying the secondary structure of proteins leads to an understanding of the components that make up a whole protein. An understanding of the structure of the whole protein is often vital to understanding its digestive behavior in animals and nutritive quality. Usually protein secondary structures include α-helix and β-sheet. The percentages of these two structures in protein secondary structures may influence feed protein quality and digestive behavior. Feathers are widely available as a potential protein supplement. They are very high in protein (84%), but the digestibility of the protein is very low (5%). The objective of this study was to use synchrotron-based Fourier transform infrared (FTIR) microspectroscopy to reveal chemical features of feather protein secondary structure within amide I at ultraspatial resolution (pixel size = 10 × 10 μm), in comparison with other protein sources from easily digested feeds such as barley, oat, and wheat tissue at endosperm regions (without destruction of their inherent structure). This experiment was performed at beamline U2B of the Albert Einstein Center for Synchrotron Biosciences at the National Synchrotron Light Source (NSLS) in Brookhaven National Laboratory (BNL), U.S. Dept of Energy (NSLS-BNL, Upton, NY). The results showed that ultraspatially resolved chemical imaging of feed protein secondary structure in terms of β-sheet to α-helix peak height ratio by stepping in pixel-sized increments was obtained. Using synchrotron FTIR microspectroscopy can distinguish structures of protein amide I among the different feed protein sources. The results show that the secondary structure of feather protein differed from those of other feed protein sources in terms of the line-shape and position of amide I. The feather protein amide I peaked at ∼1630 cm^{-1}. However, other feed protein sources showed a peak at ∼1650 cm^{-1}. By using multicomponent peak modeling, the relatively quantitative amounts of α-helix and β-sheet in protein secondary structure were obtained, which showed that feather contains 88% β-sheet and 4% α-helix, barley contains 17% β-sheet and 71% α-helix, oat contains 2% β-sheet and 92% α-helix, and wheat contains 42% β-sheet and 50% α-helix. The difference in percentage of protein secondary structure may be part of the reason for different feed protein digestive behaviors. These results demonstrate the potential of highly spatially resolved infrared microspectroscopy to reveal feed protein secondary structure. Information from this study by the infrared probing of feed protein secondary structure may be valuable as a guide for feed breeders to improve and maintain protein quality for animal use.

KEYWORDS: Synchrotron; infrared microspectroscopy; protein secondary structure; amide I; α-helix; β-sheet

INTRODUCTION

The order of the amino acids in a chain is known as its primary structure. As the amino acid chain (polypeptide) is being synthesized, it is somewhat flexible. The polypeptide can bend and twist in several ways, but it stops short of being able to flop about freely. Most polypeptide chains fold up into a stable, three-dimensional molecule shortly after synthesis. Due to interactions between chemical groups on the amino acids, a few characteristic patterns occur frequently within folded proteins. These recurring shapes are called protein secondary structure, and they occur repeatedly because they are particularly stable. The most commonly occurring protein secondary structures include the α-helix and the β-sheet (*1, 2*).

* Address correspondence to this author at the College of Agriculture, University of Saskatchewan, 6D34 Agriculture Building, 51 Campus Dr., Saskatoon, SK, Canada S7N 5A8 [telephone (306) 966-4132; e-mail yupe@sask.usask.ca].

† College of Agriculture, University of Saskatchewan.

§ Canadian Light Source.

10.1021/jf0490955 CCC: $27.50
Published on Web 11/05/2004

Studying the secondary structure of proteins leads to an understanding of the components that make up a whole protein. An understanding of the structure of the whole protein is often vital to an understanding of its digestive behavior in animals and nutritive quality.

Feathers are widely available as a potential protein supplement in the animal feed industry. There are >1 million tonnes of feathers produced each year in the United States alone, and as the consumption of poultry meat increases, so will the production of this valuable raw material. Feathers do not suffer from the disadvantages of antinutritional factors, such as tannins, glucosinolates, lectins, and trypsin-inhibiting factors (*3*). Feathers are very high in protein (84%), but the digestibility of the protein is very low (5%) (*3*). Because of feathers' high protein content, it has been of interest in nutritional studies.

The low digestibility of feather protein is related to several structural characteristics such as the high keratin content, the strong disulfide bonding of the amino acids, and the relationship of β-sheet to solubility (*3*−*6*).

Traditional analytical chemistry usually looks for a specific known component such as protein through homogenization of the tissue and separation of the components of interest (protein) from the complex matrix. As a result, information about the spatial origin and distribution of the component of interest (protein) is lost and the object of the analysis is destroyed (*7*). No structural−chemical information can be obtained from this analysis.

Recently, synchrotron-based vibrational Fourier transform infrared (FTIR) microspectroscopy has been developed as a rapid, nondestructive, noninvasive, and advanced analytical technique to reveal molecular microstructural features within biological tissues and determine tissue-localized chemical microstructure (*8*). This technique, taking advantages of synchrotron light brightness (which is usually 100−1000 times brighter than a conventional globar source and has a small effective source size) is capable of exploring the molecular chemistry within microstructures of biological samples with high signal-to-noise ratios at ultraspatial resolutions without destruction of the sample's structure (*9*−*15*).

Using a standard globar-sourced FTIR microspectroscopy cannot reveal chemical features of micro-biomaterials, which are <35−100 μm (depending on the type of FTIR microspectrometer). Using synchrotron-based FTIR microspectroscopy allows plant structural chemical features within cellular dimensions (<30 μm) to be revealed (*16*). This technique is also able to chemically define the intrinsic structure and analyze individual parts with intact biological tissues. It is able to compare the tissue (species/varieties) according to spectroscopic characteristics/functional groups/spatial distribution/chemical intensity within cellular dimensions. It also can relate feed intrinsic structures to nutrient utilization, digestive behavior, and bioavailability in animals (*16*, *17*). Therefore, synchrotron FTIR microspectroscopic imaging can be used to generate spatially localized chemical information, which can be linked to structural information (*7*). Our published results (*15*, *16*) show that with synchrotron infrared microspectroscopy, localization of protein in cereal grains was achievable from synchrotron FTIR microscopic mapping data and protein structural features could be detected from protein amide I bands (*8*).

The objectives of this study were to spatially resolve the secondary structure of protein in different feed sources using synchrotron infrared microspectroscopy and to reveal chemical features of protein secondary structure in feather microstructure in comparison with other protein sources from relatively easily digested feeds.

MATERIALS AND METHODS

Feed Protein Sources—Feather, Wheat, Oat, and Barley. Feather samples were obtained from the Poultry Centre of the Department of Animal and Poultry Science, University of Saskatchewan (Saskatoon, Canada). Wheat (cv. Superb-2001) was obtained from the Seed Increase Unit, Agriculture and Agri-Food, Canada (Indian Head, SK), which was arranged by Vern Racz (Director, Prairie Feed Source Center). Dolly Barley was supplied by the Dairy Nutrition Laboratory (Dr. David Christensen), Department of Animal and Poultry Science, University of Saskatchewan. Oat (cv. Derby) was obtained from the Crop Development Centre, University of Saskatchewan.

Synchrotron IR Slide Preparation. The feather, wheat, oat, and barley were cut into thin cross sections (~6 μm thick) using disposable razor blade microtome knives at the Western College of Veterinary Medicine, University of Saskatchewan. The unstained cross sections were mounted onto Low-e IR microscope slides (Kevley Technologies, Chesterland, OH) for synchrotron FTIR microspectroscopy in reflectance mode. More detailed methodology on slide preparation was reported by Yu et al. (*15*−*17*).

Photomicrograph of Cross Sections of Feather Tissues. Photomicrographs of cross sections of the feather tissues (thickness = 6 μm) were taken with a digital camera from the slides.

Synchrotron Light Source and FTIR Microspectroscopy. The experiment was carried out on the U2B beamline at the Albert Einstein Center for Synchrotron Biosciences in the National Synchrotron Light Source (NSLS) at Brookhaven National Laboratory (BNL) in Upton, NY. The beamline is equipped with a FTIR spectrometer (Nicolet Magna 860) with KBr beam splitter and liquid nitrogen cooled MCT detectors coupled with an IR microscope (Nic-Plan, Nicolet Instruments, Madison, WI) with Schwartzshild a 32× objective and 10× condenser. Synchrotron radiation from the VUV storage ring at beamline U2B entered the interferometer via a port of the instrument designed for use with infrared emission. The IR spectra were collected in the mid-IR range, 4000−800 cm^{-1}, at a resolution of 4 cm^{-1} with 64 scans co-added. The aperture setting was 10 × 10 μm. Stage control, spectrum data collection, and processing were performed using OMNIC 6.0 (Thermo-Nicolet, Madison, WI). Scanned visible images were obtained using a charge-coupled device (CCD) camera linked to the infrared images.

Chemical Imaging. The spectral data were collected, corrected for the background spectrum, displayed in the absorbance mode, and analyzed using OMNIC 6.0 (Spectra Tech). The data were displayed either as a series of spectroscopic images collected at individual wavelengths (1630 cm^{-1}) or as a collection of infrared spectra obtained at each pixel position in the image. Chemical imaging of β-sheet to α-helix height ratio in protein secondary structures indicated by the amide I bands (peak at ca. 1650 or 1630 cm^{-1} representing α-helix or β-sheet, respectively) (*8*, *13*) in the intrinsic structures of the feed samples was determined by the OMNIC 6.0 software (Spectra Tech) at the spectral region (1650−1550 cm^{-1}) of greatest interest. The chemical mapping of feather tissue and barley, oat, and wheat endosperm at beamline U2B provided data from which to choose spectra for modeling amide I component peaks.

Quantification of the Percentage of α-Helix and β-Sheet in Feed Protein Secondary Structures. Because protein amide I component bands were overlapped, a specific multipeak fitting or modeling procedure was required. To determine the relative amount of α-helix and β-sheet protein secondary structure, two steps were applied. The first step was using the secondary derivative in OMNIC (Thermo Nicolet) to identify protein amide I component peak frequencies. The second step was using a multipeak fitting program with Lorentz function in Origin to quantify the multicomponent peak areas in protein amide I bands. The relative amount of α-helix and β-sheet based on the modeled peak area was calculated according to the report generated by the software.

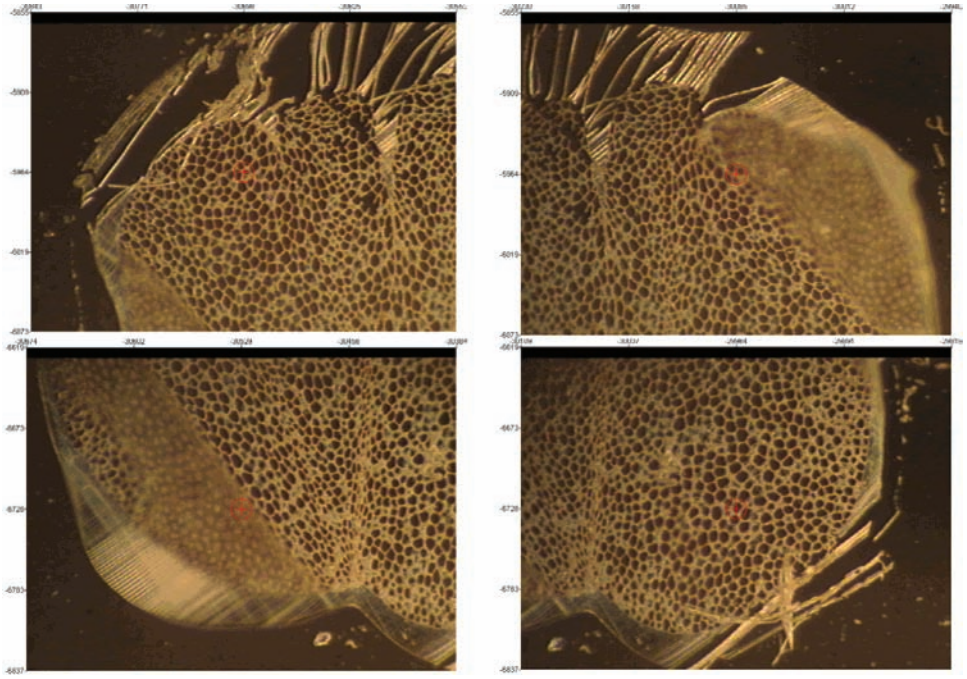

Figure 1. Photomicrograph of cross-section of the feather tissue (6 μm).

RESULTS AND DISCUSSION

Feather Photomicrograph. The photomicrographs of cross sections of the feather are presented in **Figure 1**. These photomicrographs show only the structural information, not the structural−chemical information. It is evident from these figures that there is limited chemical information available from these cross sections. They do not give information on localized structural−chemical information. Furthermore, with traditional "wet" analytical methods, it is not possible to determine chemical features of the inherent structures at ultraspatial resolution (3−10 μm) (*7*, *9*). This is because traditional analytical chemistry for the determination of feed structures relies heavily on the use of harsh chemicals and derivatization, therefore altering the native plant structures and possibly generating artifacts (*18*). Using such methods, the chemist attempts to look for a specific component through homogenization of the tissue and separation of the component of interest from the complex matrix. As a result, information about the spatial origin and distribution of the component of interest is lost (*7*).

Unique Secondary Structures of Feather Protein Indicated by Amide I Infrared Band, Compared with Other Feed Protein Sources. Typical protein secondary structures include the α-helix and β-sheet (*1*, *2*). The protein IR spectrum has two primary features, the amide I (∼1600−1700 cm^{-1}) and amide II (∼1500−1560 cm^{-1}) bands, which arise from specific stretching and bending vibrations of the protein backbone. The amide I band arises predominantly from the C═O stretching vibration of the amide C═O group. The vibrational frequency of the amide I band is particularly sensitive to protein secondary structure (*10*, *12*, *19*) and can be used to predict protein secondary structure. For α-helix, the amide I is typically in the range of 1648−1658 cm^{-1}. For β-sheet, the peak can be found within the range of 1620−1640 cm^{-1} (*19*). The amide II (predominantly an N−H bending vibration coupled to C−N stretching) is also used to assess protein conformation. However, as it arises from complex vibrations involving multiple functional groups, it is less useful for protein structure prediction than the amide I band (*20*).

Figure 2 illustrates unique line-shapes and positions of protein amide I in mid-IR from the different protein sources (feather protein versus barley, oat, and wheat protein) at ultraspatial resolution. The results show that the intrinsic structures (pixel size = 10 × 10 μm) of amide I from feather, barley, wheat, and oat proteins were different. The feather protein amide I peaks at ∼1630 cm^{-1}, but barley, wheat, and oat protein sources show a peak at ∼1650 cm^{-1}. These results indicate that feather contains a higher percentage of β-sheet but a lower percentage of α-helix in the protein secondary structures on a relative basis. However, barley, wheat, and oat contain lower percentages of β-sheet but higher percentages of α-helix. This may cause different protein values between the feed proteins with a poor protein value of feathers. To improve feather protein value, one possibility is to alter the ratio of β-sheet to α-helix in feather protein secondary structures by processing or treatment to improve access of digestive enzymes to protein structures.

Ultraspatially Resolved Chemical Mapping of Protein Amide I β-Sheet to α-Helix Ratio. Biological component ratio images showing structural chemical features can be obtained by the height or area under one functional group band divided by the height or area under another functional group band at each pixel. **Figure 3** represents color maps of protein amide I β-sheet to α-helix ratio in feather tissue and barley, oat, and wheat endosperm tissue and single-pixel spectra measuring an area as small as 10 × 10 μm of the sample, which is within the cellular dimension. It shows visible and chemical images in false-color representation of the chemical functional group amide I intensities and spectra at various pixels. Using synchrotron FTIR microspectroscopy, the distribution and relative concentration of the chemical components associated with the inherent ultrastructure were mapped. **Figure 3** shows the area under the ∼1630 cm^{-1} peak height to ∼1650 cm^{-1} peak height ratio mapping attributed to β-sheet and α-helix absorption ratio (amide I).

Component ratio mapping has two advantages. The first one is that using those ratios, any spectral intensity variations due to tissue thickness changes are eliminated. The second one is that the ratio maps are able to indicate relative tissue component

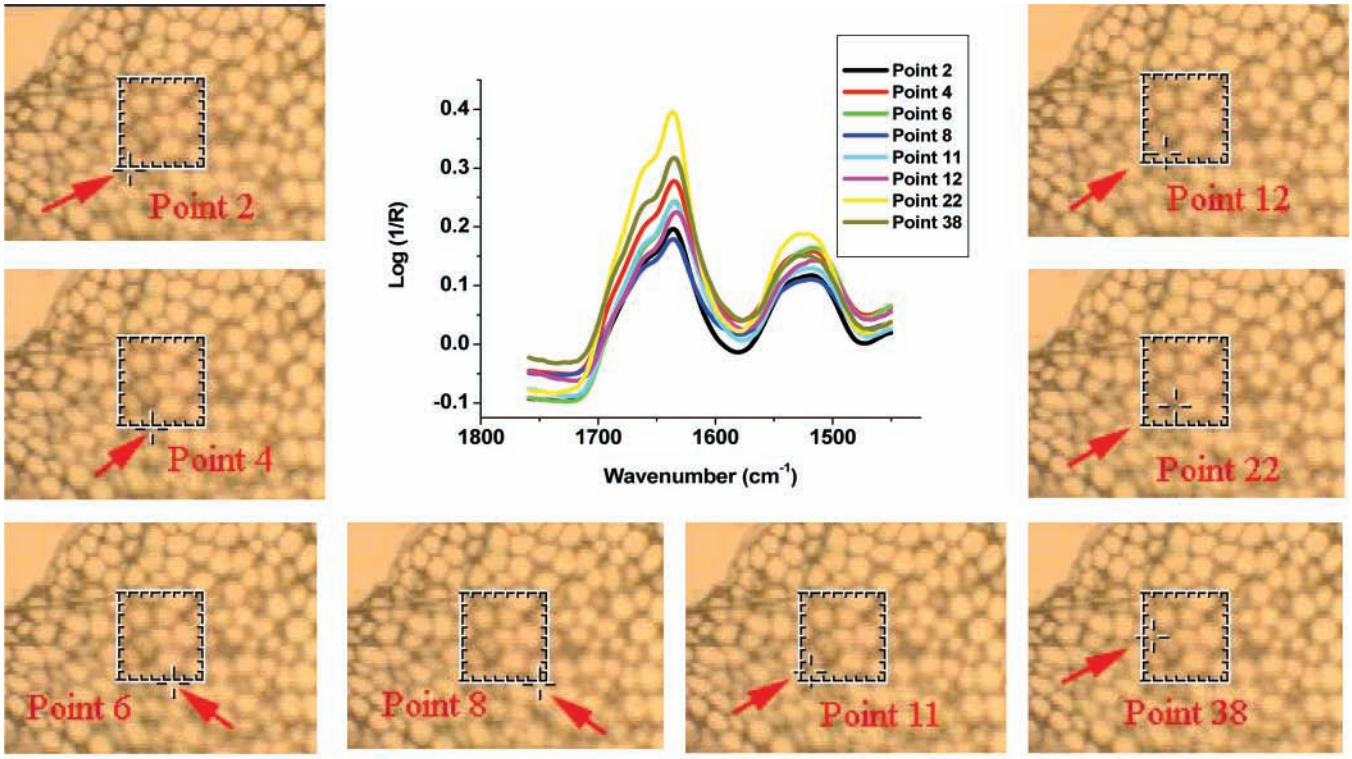

(a): feather protein

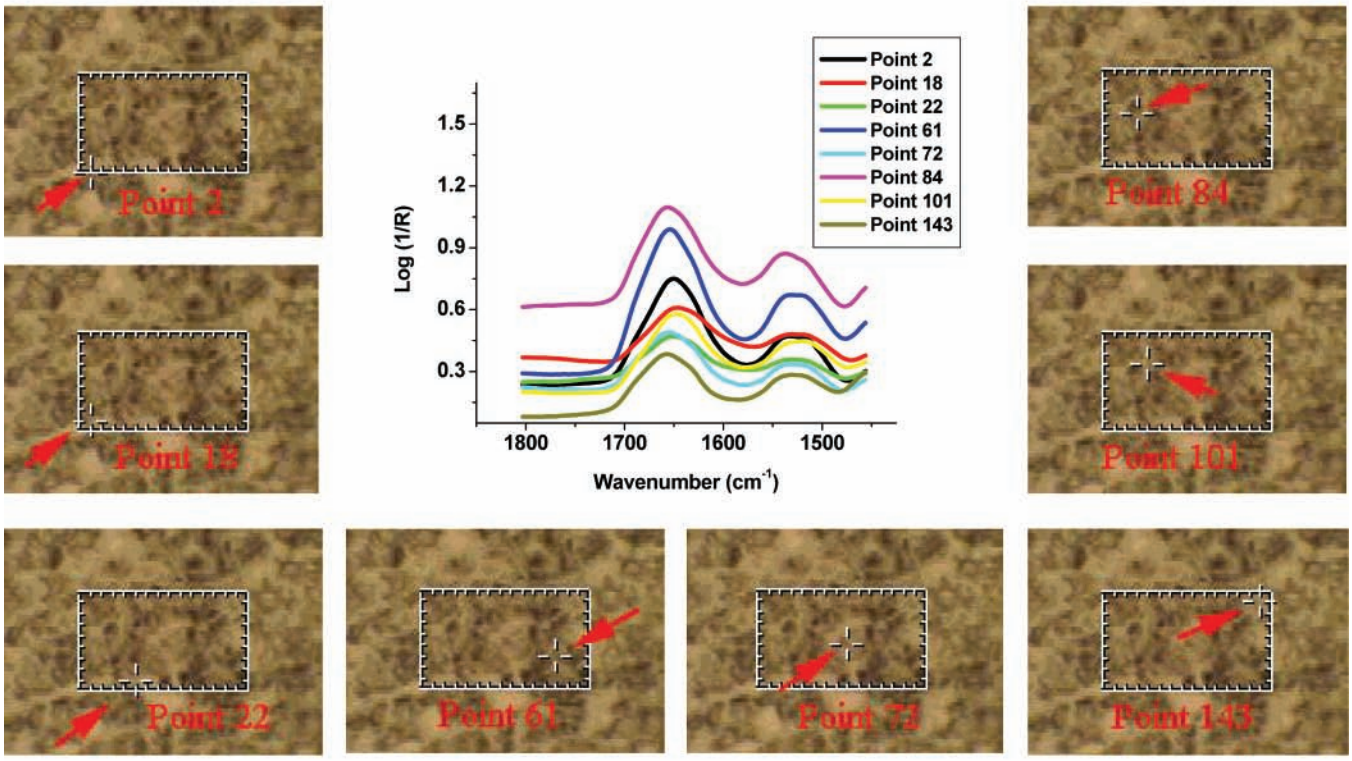

(b): barley Protein

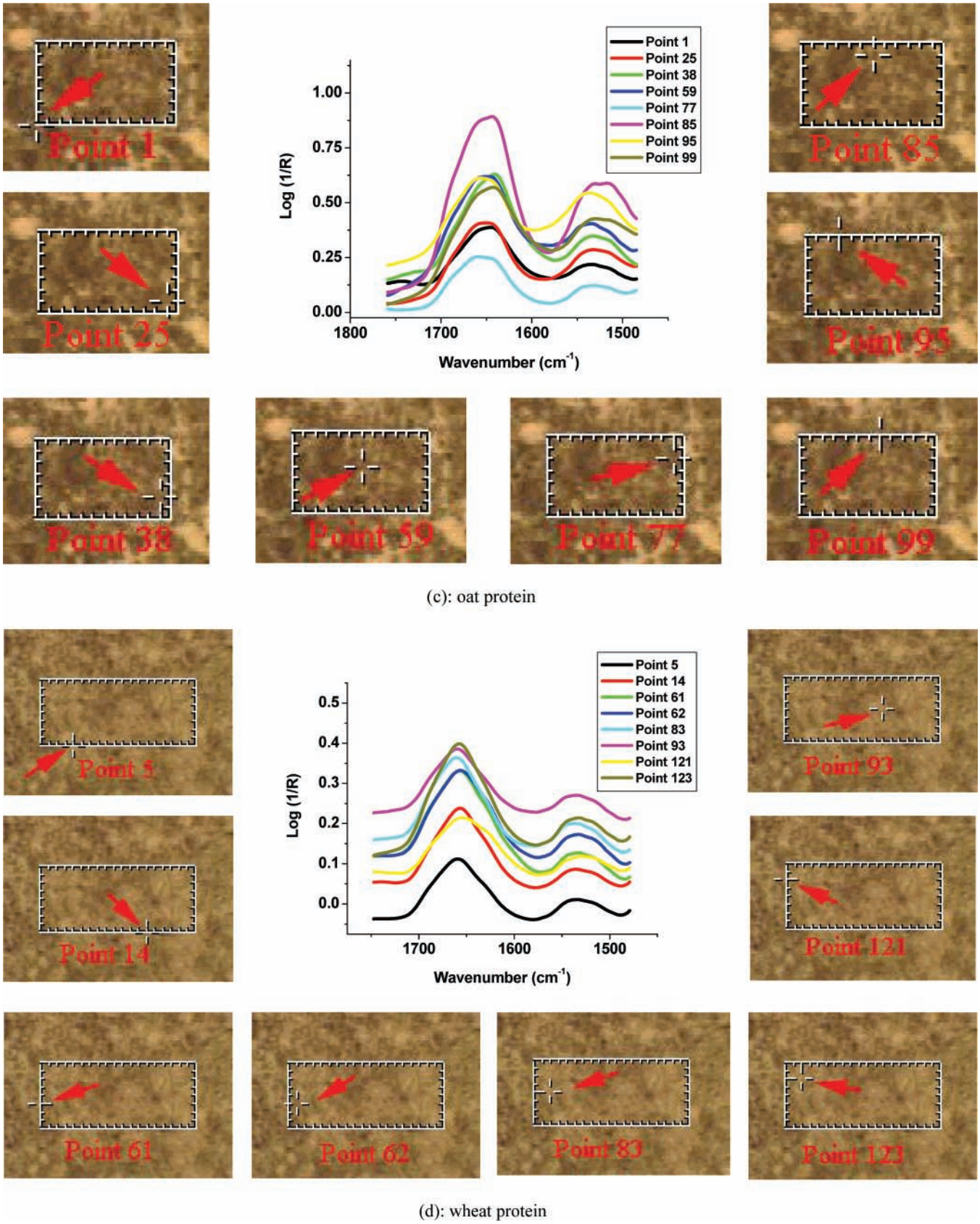

Figure 2. Lineshape and position of feed protein amide I (**a**) from feather protein, (**b**) from barley protein, (**c**) from oat protein, and (**d**) from wheat protein, respectively, indicating different protein secondary structures among protein sources (α-helix at $\sim$1650 cm^{-1} and β-sheet at $\sim$1630 cm^{-1}). (The second peaks are protein amide II; the peak heights from different points were different due to separation of each peak for each point in order for people to read the peaks clearly.)

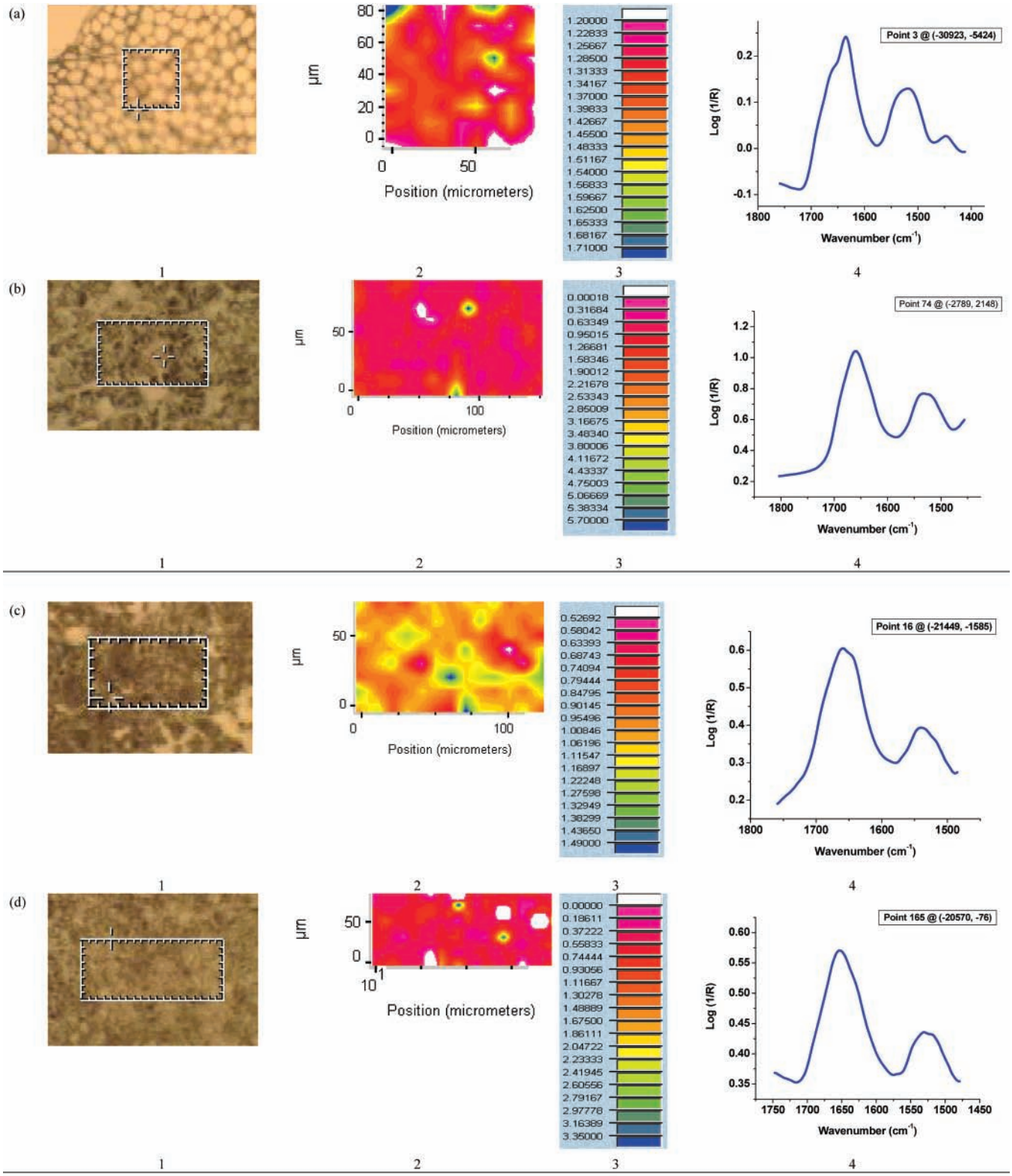

Figure 3. Functional group ratio images of the feather tissue (**a**), barley endosperm (**b**), oat endosperm (**c**), and wheat endosperm (**d**): 1, visible image; 2, chemical image; 3, chemical intensity; 4, spectra corresponding to the pixel at the cross-hair in the visible image; 1b, area under 1630 cm^{-1} peak height divided by 1650 cm^{-1} peak height showing protein amide I β-sheet to α-helix ratio distribution. (Some holes and blue "hot spots" were due to artifacts during the mapping.)

contents, which could be used to determine food or feed quality, characteristics, and nutritive values and in plant breeding programs. Component ratio mapping can be used to compare different feed varieties according to the inherent structural spectral characteristics, chemical functional group intensity, and distribution (e.g., seed coat features, pericarp features between different seed varieties). It can be used to chemically define the feed intrinsic structure and analyze individual feed structure with intact tissue (*16*).

Our results demonstrate the potential of highly spatially resolved infrared microspectroscopy to reveal cereal grain and other feed protein secondary structure.

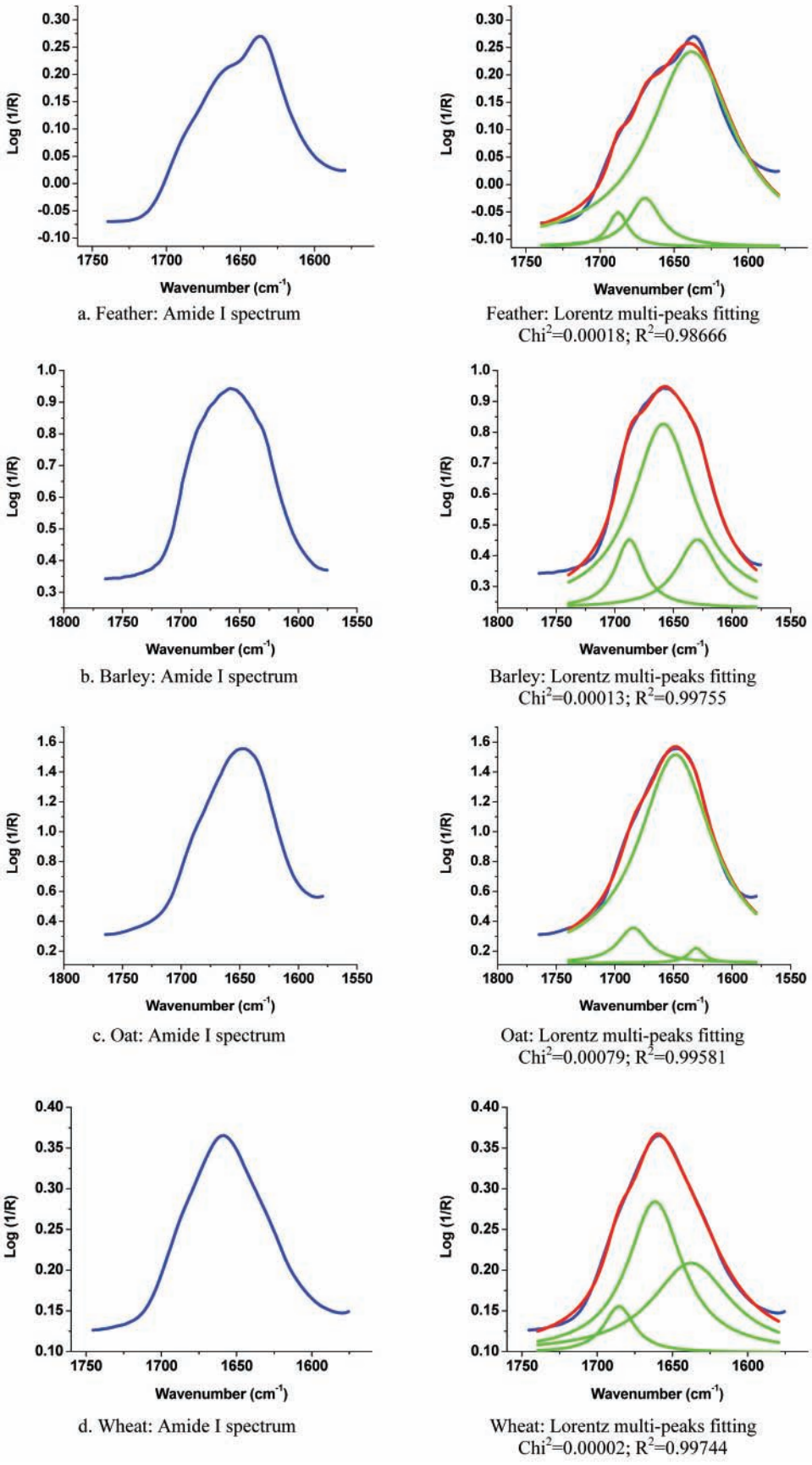

Figure 4. Multicomponent amide I peak modeling showing feather (**a**) containing ca. 88% β-sheet and 4% α-helix; barley (**b**) containing ca. 17% β-sheet and 71% α-helix; oat (**c**) containing ca. 2% β-sheet and 92% α-helix; and wheat (**d**) containing ca. 42% β-sheet and 50% α-helix. (Method of multicomponent modeling: step 1, using secondary derivative in OMNIC to identify amide I component peak frequencies; step 2, using multipeak fitting program with Lorentz function in origin to quantify the multicomponent peak areas in protein amide I region.)

Modeling of Protein Amide I Peaks to Quantify the Percentage of Protein Secondary Structures (α-Helix, β-Sheet). Because feed protein amide I component peaks overlay each other, the secondary derivative was used to identify amide I component peak frequencies, and then multicomponent peak fitting with Lorentz function was used to quantify the multicomponent peak area in the protein amide I region. **Figure 4** shows that feathers contained ca. 88% β-sheet and 4% α-helix, barley contained ca. 17% β-sheet and 71% α-helix, oat contained ca. 2% β-sheet and 92% α-helix, and wheat contained ca. 42% β-sheet and 50% α-helix. The difference in percentage of protein secondary structure may be partly responsible for different feed protein digestive behaviors. Wetzel et al. (*8*) compared hard wheat cultivars (including red, white, winter, and spring wheats grown at different locations) and soft wheat cultivars and found that hard wheat contained, roughly, 40−60% α-helix and 25−30% β-sheet and soft wheat contained around 40% α-helix and 40% β-sheet (obtained from their data). The results show hard wheat had a greater relative amount of α-helix than soft wheat. Our results showed that the wheat (cv. Superb-2001) contained ca. 42% β-sheet and 50% α-helix. The peak area ratios of α-helix to β-sheet for the hard wheat cultivars were 1.57−2.10, compared to the ratios from 0.96 to 1.07 for the soft wheat cultivars. Our results showed that the peak area ratio of α-helix to β-sheet for the wheat (cv. Superb-2001) was 1.18. However, no published results have been found for oat and barley. It is necessary to mention that our results should be considered as typical and not average for the individual seed. Many factors will affect the quality of feeds, such as location, climate, and growth conditions. Information from this study by the infrared probing of feed protein secondary structure may be valuable as a guide for feed breeders to improve and maintain protein quality for animal use. Our results demonstrate the potential of highly spatially resolved infrared microspectroscopy to reveal cereal grain and other feed protein secondary structure.

Conclusions. With synchrotron-based FTIR microspectroscopy, the ultrastructrual−chemical makeup characteristics could be revealed at a high ultraspatial resolution. Synchrotron-based FTIR microspectroscopy revealed that the secondary structure of feather protein differed from that of other feed protein sources in terms of the line shape and position of amide I in mid-IR within the cellular dimension. By using multicomponent peak modeling, the relative quantitatiion of protein amide I component peaks—α-helix and β-sheet—could be resolved. The results indicated that the secondary structure of feather protein contains a higher percentage of β-sheet and a lower percentage of α-helix on the relative basis, compared to the grain protein sources. This may be part of the reason for feather's poor protein value in comparison with other feed protein sources. Our results demonstrate the potential of highly spatially resolved infrared microspectroscopy to reveal feed protein secondary structure. Further study is needed to quantify the relationship between protein secondary structure and digestive behavior of various varieties of grain feed protein sources such as barley, oat, and wheat.

ACKNOWLEDGMENT

We are grateful to Ned Marinkovic and Lisa Miller (NSLS-BNL, Upton, NY) for helpful data collection at the U2B experimental station and Vern Racz (Prairie Feed Resource Center, University of Saskatchewan) for providing feed samples. Canadian Light Source Inc. (CLS, national synchrotron facility) has a mutual agreement with the National Synchrotron Light Source for use of the synchrotron beam at The National Synchrotron Light Source, U.S. Department of Energy.

LITERATURE CITED

(1) Dyson, H. J.; Wright, P. E. Peptide conformation and protein folding. *Curr. Opin. Struct. Biol.* **1990**, *3*, 60−65.

(2) Carey, F. A. *Organic Chemistry*, 3rd ed.; McGraw-Hill: New York, 1996.

(3) Chandler, N. J. Dairy Cattle—Feather meal: Its nutritional value and use in dairy and beef rations. Retrieved in Nov 2003 from http://www.engormix.com/e_articles_dairy_cattle.asp?ID=79.

(4) Ward; Lundgren, H. P. Formation, composition and properties of keratins. *Adv. Protein Chem.* **1954**, *9*, 244−297.

(5) Fraser, R. D. B.; MaCrae, T. P.; Rogers, G. E. Keratins: their composition, structure, and biosynthesis, Fraser, R. D. B., Ed.; Thomas: Springfield, IL, 1972.

(6) Greg, K.; Rogers, G. E. Feather keratin; Composition, structure and biogenesis. In *Biology of Integuments*; Springer-Verlag: Berlin, Germany, 1986; Vol. 2.

(7) Budevska, B. O. Vibrational Spectroscopy Imaging of Agricultural Products. In *Handbook of Vibrational Spectroscopy*, Chalmers, J. M., Griffiths, P. R., Eds.; John Wiley and Sons, Inc.: New York, Vol. 5, pp 3720−3732.

(8) Wetzel, D. L.; Srivarin, P.; Finney, J. R Revealing protein infrared spectral detail in a heterogeneous matrix dominated by starch. *Vib. Spectrosc.* **2003**, *31*, 109−114.

(9) Wetzel, D. L.; Eilert, A. J.; Pietrzak, L. N.; Miller, S. S.; Sweat, J. A. Ultraspatially resolved synchrotron infrared microspectroscopy of plant tissue in situ. *Cell. Mol. Biol.* **1998**, *44*, 145−167.

(10) Miller, L. M. The impact of infrared synchrotron radiation on biology: past, present, and future. *Synchrotron Radiat. News* **2000**, *13*, 31−37.

(11) Holman, Hoi-Ying N.; Bjornstad, K. A.; McNamara, M. P.; Martin, M. C.; McKinney, W. R.; Blakely, E. A. Synchrotron infrared spectromicroscopy as a novel bioanalytical microprobe for individual living cells: cytotoxicity considerations. *J. Biomed. Optics* **2002**, *7*, 1−10.

(12) Marinkovic, N. S.; Huang, R.; Bromberg, P.; Sullivan, M.; Toomey, J.; Miller, L. M.; Sperber, E.; Moshe, S.; Jones, K. W.; Chouparova, E.; Lappi, S.; Franzen S.; Chance, M. R. Center for Synchrotron Biosciences' U2B beamline: an international resource for biological infrared spectroscopy. *J. Synchrotron Radiat.* **2002**, *9*, 189−197.

(13) Miller, L. M. Infrared Microsperctroscopy and Imaging. Retrieved in October 2002 from http://nslsweb.nsls.bnl.gov/nsls/pubs/nslspubs/imaging0502/irxrayworkshopintroduction.ht.

(14) Yu, P.; McKinnon, J. J.; Christensen, C. R.; Christensen, D. A. Mapping plant composition with synchrotron infrared microspectroscopy and relation to animal nutrient utilization. In *Proceedings of the Canadian Society of Animal Science Conference*, University of Saskatchewan, Saskatoon, SK, Canada, June 10−13, 2003; pp 1−20 (Invited Article and Conference Speech).

(15) Yu, P.; McKinnon, J. J.; Christensen, C. R.; Christensen, D. A.; Marinkovic, N. S.; Miller, L. M. Chemical Imaging of Micro-Structures of Plant Tissues within Cellular Dimension Using Synchrotron Infrared Microspectroscopy. *J. Agric. Food Chem.* **2003**, *51*, 6062−6067.

(16) Yu, P.; McKinnon, J. J.; Christensen, C. R.; Christensen, D. A. Using synchrotron transmission FTIR microspectroscopy as a rapid, direct and nondestructive analytical technique to reveal molecular microstructural-chemical features within tissue in grain barley. *J. Agric. Food Chem.* **2004**, *52*, 1484−1494.

(17) Yu, P.; Christensen, D. A.; Christensen, C. R.; Drew, M. D.; Rossnagel, B. G.; McKinnon, J. J. Use of Synchrotron FTIR Microspectroscopy to Identify Chemical Differences in Barley Endosperm Tissue in Relation to Rumen Degradation Characteristics. *Can. J. Anim. Sci.* **2004**, *84* (3), 523−527.

(18) Stewart, D.; McDougall, G. J.; Baty, A. Fourier transform infrared microspectroscopy of anatomically different cells of flax (*Linum usitatissimum*) stems during development. *J. Agric. Food Chem.* **1995**. *43*, 1853−1858.

(19) Martin, M. C. Fourier-Tranform Infrared Spectroscopy. Retrieved in October 2002 from http://infrared.als.lbl.gov/.
(20) Jackson, M., Mantsch, H. H. Infrared spectroscopy Ex Vivo Tissue Analysis. In *Biomedical Spectroscopy*, 2000, pp 131−156.

Received for review June 3, 2004. Revised manuscript received September 13, 2004. Accepted September 17, 2004. This research has been supported by grants from the Saskatchewan Agricultural Development Fund (ADF). The National Synchrotron Light Source in the Brookhaven National Laboratory (NSLS-BNL, Upton, NY) is supported by the U.S. Department of Energy, Contract DE-AC02-98CH10886.

JF0490955